Mechanistic Studies of Continuous Glucose Upgrading Over Lewis Acidic Silicates by Operando UV-Vis and HSQC NMR

Botti, Luca; Meier, Sebastian; Hammond, Ceri

Published in:
A C S Catalysis

Link to article, DOI:
10.1021/acscatal.0c03638

Publication date:
2021

Document Version
Peer reviewed version

Mechanistic Studies of Continuous Glucose Upgrading Over Lewis Acidic Silicates by Operando UV-Vis and HSQC NMR

Journal:	*ACS Catalysis*
Manuscript ID	cs-2020-036382.R2
Manuscript Type:	Article
Date Submitted by the Author:	12-Dec-2020
Complete List of Authors:	Botti, Luca; Imperial College London, Department of Chemical Engineering Meier, Sebastian; Technical University of Denmark, Department of Chemistry Hammond, Ceri; Imperial College London, Department of Chemical Engineering

Mechanistic Studies of Continuous Glucose Upgrading Over Lewis Acidic Silicates by *Operando* UV-Vis and HSQC NMR

Luca Botti,[1] Sebastian Meier[2] and Ceri Hammond[1]*

[1]Department of Chemical Engineering, Imperial College London, London, SW7 2AZ, UK

[2]Department of Chemistry, Technical University of Denmark Kemitorvet, Bygning 207, 2800 Kgs. Lyngby, Denmark

E-mail: ceri.hammond@imperial.ac.uk

Keywords Operando spectroscopy · UV-Vis · Glucose · Zeolites · Continuous · Acid catalysis

Abstract: Lewis acidic silicates are effective catalysts for the conversion of glucose to bio-molecules of industrial interest, such as methyl lactate and methyl vinyl glycolate. Although well studied in recent years, open questions of these processes remain, particularly in regards to elements of the reaction mechanisms, and how the catalysts deactivate during continuous operation. Such questions endure due to the lack of spectroscopic techniques capable of providing insight into the catalytic reaction at operational conditions. In this study, we follow the catalytic conversion of glucose over the Lewis acidic silicates Sn-Beta and Hf-Beta in a continuous flow reactor equipped with operando UV-Vis spectroscopy. In doing so, we identify several transient absorption features related to the activation and conversion of glucose at various operational conditions (<170 °C, <25 bar). Additional spectroscopic studies (high-field ^{1}H-^{13}C HSQC NMR) and kinetic cross-experiments allow each Sn-glucose interaction to be assigned to a particular class of product, and hence to various selective or non-selective reaction pathways. Based on these assignments, *operando* UV-Vis is used to probe how partial deactivation of the stannosilicate catalyst affects the overall performance of the glucose upgrading reaction during continuous operation. We demonstrate how deactivation during glucose conversion is non-uniform, with different reaction pathways losing activity at different rates. These findings are shown to have consequences with respect to improving the selectivity of catalysts for glucose upgrading during continuous operation.

Introduction

Climate change coupled with population increase lends urgency to the development of environmentally sustainable processes for material and energy production.[1-3] In this regard, the exchange of fossil feedstock with renewable sources of energy and carbon is a major target. Biomass shows potential as a sustainable feedstock for the production of important platform molecules, particularly when it can be converted to useful products by scalable chemo-catalytic methods.[4,5] Of particular importance is the catalytic conversion of glucose, since glucose is the primary product of CO_2 fixation and is the most common sugar gathered from agricultural waste biomass.[6,7]

One of the most promising catalysts for catalytic glucose conversion is Sn-Beta.[8-12] Sn-Beta is a microporous zeolite in which tin atoms are isomorphously substituted into the otherwise siliceous Beta zeolite structure, where they behave as Lewis acid centres capable of activating and converting glucose.[8-12] A previous study by Tolborg *et al.*[13] demonstrated that Sn-Beta can produce a variety of different terminal products starting from glucose, including: *trans*-2,5,6-trihydroxy-3-hexenoic methyl ester (THM) and furanics such as 5-(hydroxymethyl)furfural (HMF), all of which are derived from β-dehydration of 3-deoxyglucosone (3-DG) (β-dehydration products); methyl lactate (ML) and methyl vinyl glycolate (MVG), derived from retro-aldol cleavage of hexoses (RA products); fructose and mannose, as products of glucose isomerization (GI products); methyl-glycosides, by alkylation of the monosaccharides in solution (alkylation products); and finally 3-deoxy-γ-lactones (3DGL), formed upon ring closure of 3DG (Scheme 1).[13] Whilst the ability of Sn-Beta to catalyse so many reactions makes it a very interesting catalyst, it also makes control of the selectivity of the catalyst towards a specific chemical pathway very challenging. This is especially problematic in the context of process design, process economics and sustainable carbon management.

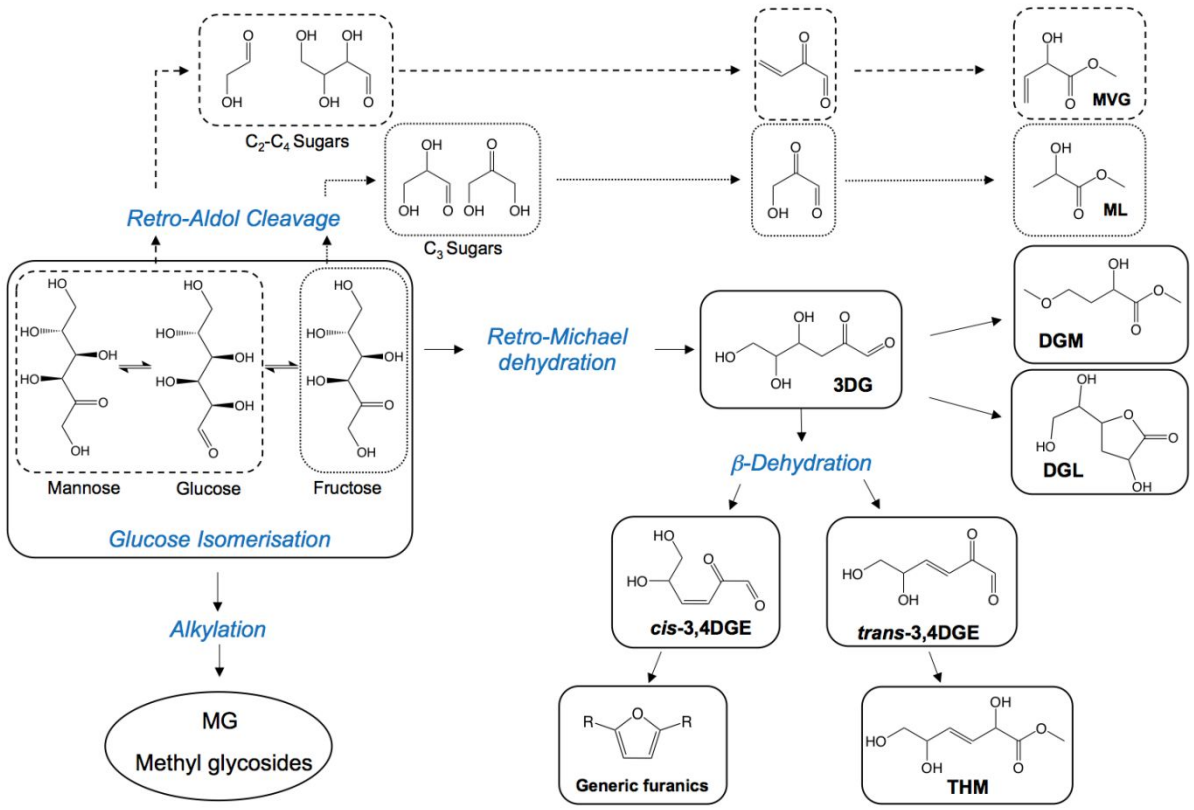

Scheme 1. Schematic representation of the reactions catalysed by Sn-Beta during glucose upgrading.

Although experimental works have shown that the catalyst composition, preparation methodology and reaction conditions (temperature, presence of alkali and/or water) can impact the final product distribution attained when converting glucose over Sn-Beta,[13-16] few studies have addressed how the substrate (in this case glucose) interacts with the catalyst at operative conditions,[13,17] or how to monitor the competition amongst these chemical pathways in the reaction environment.

A major obstacle towards addressing these open questions is the lack of spectroscopic insight into the operating catalytic reaction. In particular, the conditions at which glucose upgrading is carried out (liquid phase, 80-170°C, <25 bar when operating continuously[15]) makes *in situ* study of this system challenging. Consequently, existing spectroscopic and mechanistic studies of this system have relied on the correlation of kinetic data to various *ex situ* methodologies (*e.g.* MAS NMR),[18-20] and/or to probe molecule studies that monitor the interaction of Sn-Beta with model compounds such as CD_3CN and pyridine.[21-25] An additional source of difficulty is that several of the compounds generated by Sn-Beta during these processes (Scheme 1) are not amenable to detection by routine chromatographic

analyses, meaning that low carbon balances are usually reported. Together, these hurdles have made it difficult to understand the types of interaction that can occur between Sn and glucose, and how these interactions result in competing reaction pathways.[26]

In this manuscript, we follow the upgrading of glucose over several Sn- and Hf-silicate catalysts by *operando* UV-Vis spectroscopy.[27] This technique is performed at operational conditions (*in operando,* <150 °C, <25 bar) and is carried out in continuous flow, which allows simultaneous study of the deactivation of these interactions as a function of time on stream. To benchmark the UV-Vis absorptions detected in the *operando* reactor, high-field liquid-state NMR measurements (^{1}H-^{13}C HSQC) are used to cross-correlate the optical intermediates to various products in solution, permitting each feature to be assigned to a particular class of reaction product and hence reaction pathway.[26,28] Based on these findings, we later monitor the deactivation of stannosilicate catalysts for glucose conversion, allowing the deactivation of different reaction pathways to be monitored selectively during continuous operation.

Results and Discussion

Identification of optical intermediates by *operando* UV-Vis spectra

As described above, Sn-Beta is known to catalyse several selective and non-selective reaction pathways starting from glucose (Scheme 1).[13] Although various reaction stimuli – including choice of catalyst, method of preparation and presence of additives in the reaction solution (particularly alkali and water)[14-16] – affect the course of the glucose conversion reaction over Sn-Beta, a dominating factor with respect to progress of the reaction is the choice of operational temperature.[13,15] In particular, it has been established that GI is the dominant selective reaction pathway at temperatures of up to 110 °C, whereas RA processes become dominant as the temperature is increased beyond 110 °C.[13,15]

Accordingly, preliminary *operando* UV-Vis studies were focused upon monitoring the conversion of glucose over Sn-Beta at various temperatures between 80 and 140 °C (see Supporting Information Figures S1-S3 for further details on the reactor). Each *operando* experiment was performed with a

feed solution of 1 wt. % glucose in methanol, and identical flow rates (0.75 mL min^{-1}) and masses of catalyst (0.1 g catalyst) were employed in each experiment. Each individual experiment was performed with a fresh sample of catalyst, which in the case of these preliminary experiments was a sample of Sn-Beta containing 10 wt. % Sn, and which was prepared by Solid State Incorporation (henceforth 10Sn-$Beta_{SSI}$).[29] Spectra were recorded after 0.5 h of time on stream to minimise the impact of catalyst deactivation, and all spectra were background corrected to the spectrum of the catalyst in a flow of pure methanol, *i.e.* to the state of the catalyst prior to introduction of glucose. The *operando* UV-Vis spectra generated by these reactions are illustrated in Figure 1. Due to the lack of extinction coefficient values for these intermediates, relative comparisons of intensity as a function of reaction perturbation were used for comparative purposes.

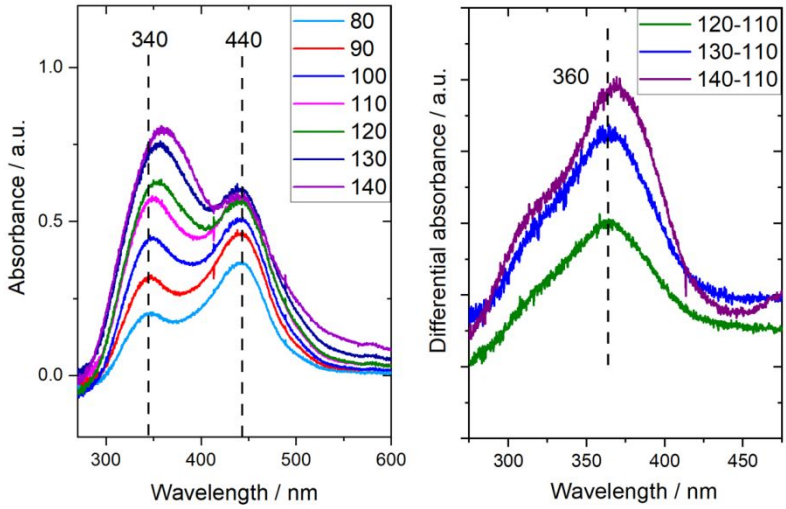

Figure 1. (Left) *Operando* UV-Vis for glucose conversion over 10Sn-$Beta_{SSI}$ between 80-140 °C. (Right) Differential *operando* UV-Vis spectrum in the 250-450 region, achieved by subtracting the spectrum of the experiment at 110 °C from those generated between 120-140 °C. Reaction conditions: 1 wt. % glucose in methanol, 0.75 mL min^{-1}, 0.1 g catalyst, various reaction temperatures between 80-140 °C.

As can be seen in Figure 1, several absorption intermediates were generated during the interaction of glucose and 10Sn-$Beta_{SSI}$. At the lowest temperature studied (80 °C), spectra consisted of two major absorptions, centred at λ = 340 nm and 440 nm (henceforth, λ_{340} and λ_{440}). However, the behaviour of these features as a function of temperature differed substantially. The λ_{440} absorption was the most intense feature observed at 80 °C, but increased only marginally upon increasing the temperature from 80 to 110 °C, after which the intensity of the feature plateaued further. In contrast, the λ_{340} absorption

was present at a much lower intensity at 80°C, but increased steeply at higher temperatures, reaching its maximum intensity at 140 °C (Figure 1, left). Alongside these changes was an evident shift in the position of the λ_{340} feature upon increasing the temperature beyond 110 °C. Analysis of the differential spectra generated by subtraction of the 110 °C spectrum from those generated at higher temperature (Figure 1, right) revealed that this shift was caused by the generation of a new contribution at λ_{360}.

Control experiments confirmed that the absorptions described in the previous section were only generated when glucose and Sn were both present in the system.[15] Specifically, these absorptions were not formed when methanol was flowed over Sn-Beta, or when the reaction solution (1 wt. % glucose in methanol) was flowed over Sn-free zeolite Beta (Figure S4), meaning that the co-presence of Sn and substrate is paramount for these absorptions to arise. [15] To verify that these absorptions did not simply arise through formation of a chromophoric (by-)product of the reaction, the reaction effluent and standards of glucose and High Fructose Corn Syrup (HFCS, 42 % glucose) were also monitored by *ex situ* UV-Vis (SI Figure S5). Interestingly, whilst the reaction effluent showed a broad absorption at high energy (250-300 nm) - confirming the presence of some chromophoric by-product in the reaction solution - none of these solutions exhibited absorptions at 340 nm and 440 nm. As the λ_{340} and λ_{440} bands were only formed in the presence of glucose and Sn, but did not relate to individual compounds formed during reaction, they can be assigned to absorbing species present due to the interaction between Sn and glucose. To further verify this, additional *ex situ* UV-Vis analyses were performed on Sn-Beta samples removed from the reactor following glucose upgrading in methanol (SI Figure S6). These measurements revealed that the absorption features described above were still visible on the catalyst even after its removal from the reaction environment, verifying that they are related to catalyst-substrate interactions (SI Figure S6).

To determine the relevance of the findings from Figure 1, the reaction effluent of each experiment was analysed by classic chromatographic techniques (HPLC-ELSD/UV and GC-FID, Figure 2). Although all of the products detected by chromatographic techniques were generated by the Lewis acid active sites of the catalyst (no products were observed when Sn-free zeolite Beta was used as catalyst), and hence are examples of selective reaction products, they can be further categorised as GI products (fructose, mannose) and RA products (ML and MVG).[13]

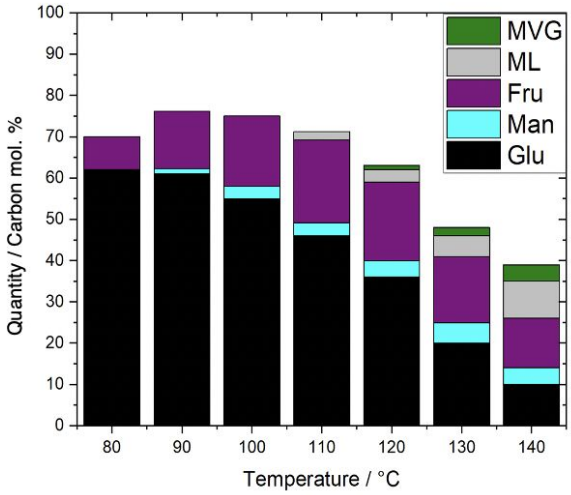

Figure 2. Yields of fructose, mannose (GI products), methyl lactate and methyl vinyl glycolate (RA products) achieved during the conversion of glucose by 10Sn-Beta$_{SSI}$ at various temperatures. Reaction conditions: 1 wt. % glucose in methanol, 0.75 mL min^{-1}, 0.1 g catalyst, various reaction temperatures between 80-140 °C.

At lower temperatures (80-110 °C), GI products were the dominant products in the reaction effluent, the yields of which increased from 7 % at 80 °C, to 26 % at 110 °C (Figure 2). However, even at these low temperatures, a substantial decrease in carbon balance was observed. This loss of carbon balance suggests that by-products not amenable to chromatographic analysis were already present in the effluent even at low temperature. Notably, the carbon balance in each of the low temperature reactions was comparable (*ca.* 75 %), indicating that the by-products formed at low temperature were not strongly impacted by the choice of temperature in this range.

Interestingly, although raising the temperature above 110 °C resulted in a substantial increase in the quantity of substrate converted – which increased from 55 % at 110 °C to >90 % at 140 °C – the overall yield of selective products (GI+RA) increased only slightly from 26 % to 30 %. Accordingly, a second major loss of carbon balance was observed in the higher temperature regime (>110 °C), the onset of which coincided with the generation of λ_{360} feature (Figure 1, right). Alongside this loss of carbon balance, the distribution of selective products also changed in the higher temperature regime, and RA products accounted for an increasing fraction of the selective products in the effluent. Figure 2 thus confirms that the cumulative yield of the products, the distribution of products between GI and

RA, the overall carbon balance (and hence, quantity of by-products), and the intensity of the *operando* UV-Vis absorbances, all strongly depend upon the reaction temperature.

To gain further insight, the evolution of the *operando* UV-Vis spectra as a function of time on stream was investigated. In particular, *operando* spectra of the glucose conversion reaction at 110 °C were recorded at several stages of a 13 h continuous reaction period. This temperature was chosen as it provided a balance between the maximal yield of desired products (GI+RA), the carbon balance of the process, and the presence of all absorption features.

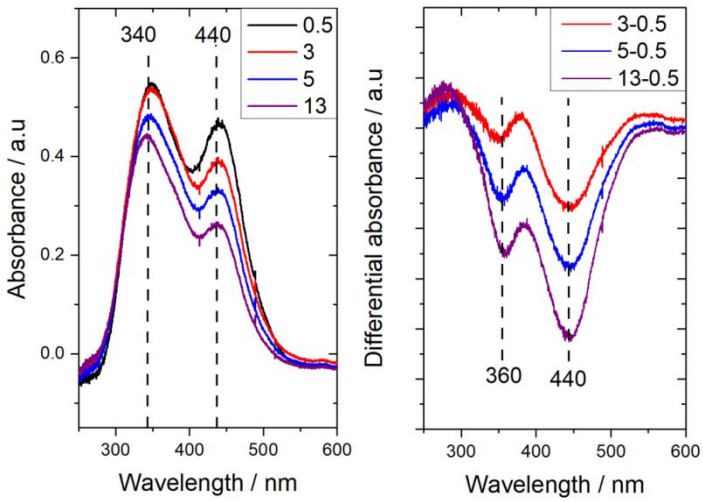

Figure 3. (Left) *Operando* UV-Vis spectra from the glucose conversion reaction catalysed by 10Sn-Beta$_{SSI}$ at 110 °C, recorded at various points of time on stream (0.5, 3, 5 and 10 h). (Right) Differential *operando* UV-Vis spectra in the 250-600 nm region, obtained by subtracting the spectrum recorded at 0.5 h on stream from those at later points of time. Reaction conditions: 1 wt. % glucose in methanol, 0.75 mL min^{-1}, 0.1 g catalyst, 110 °C.

As can be seen (Figure 3, left), over the course of 13 h on stream, the absorptions present in the *operando* UV-Vis spectra decreased in intensity. However, the rate of decrease differed markedly for the different bands in the spectra, as the λ_{440} signal lost intensity more rapidly than the λ_{340} signal (SI Figure S7). Moreover, the λ_{340} band also shifted towards higher energy, suggesting a non-uniform loss of intensity in the 330-380 nm region. To clarify the changes observed as a consequence of time on stream, differential spectra were generated by subtracting the spectrum recorded at 0.5 h on stream from those collected at later times (Figure 3, right). Consequently, signals that diminish in intensity over the relevant time period appear negative as a consequence of subtracting the spectrum at time 0.5

hours from each spectrum at time *"t"*. This analysis revealed that the λ_{340} band was a congested feature of an absorbance at approximately 330 nm (henceforth λ_{330}), and a second absorbance at 360 nm (λ_{360}), which deactivated much faster over the first 10 hours of the reaction. This finding indicates that although the λ_{360} feature observed in Figure 1 grows in strongly at higher temperatures, it was already present at 110 °C, accounting for the progressive shift of the maxima to higher wavelengths at increasing temperature. As a consequence of the loss of intensity at 360 and 440 nm, the λ_{330} UV-Vis band became the most dominant after 10 h on stream, with the majority of its intensity remaining after this operational period.

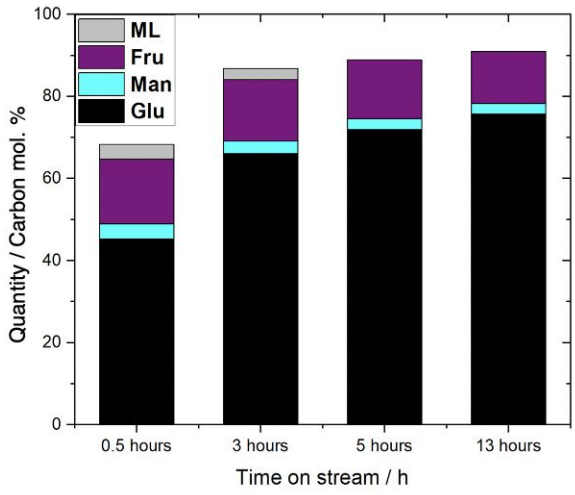

Figure 4. Kinetic data related to the conversion of glucose over 10Sn-$Beta_{SSI}$ at 110 °C at various points of time on stream (0.5, 3, 5 and 13 h). Reaction conditions: 1 wt. % glucose in methanol, 0.75 mL min^{-1}, 0.1 g catalyst, 110 °C.

Quantitative analysis of the reaction effluent revealed that the yield of selective products (GI+RA) decreased only slightly from 22 % to 16 % (Figure 4) over the 13 h reaction period. However, the quantity of glucose converted by the catalyst decreased much more dramatically, from 55 % at 0.5 h to 22 % at 13 h). As a consequence, the carbon balance of the reaction increased substantially over the first 13 h on stream (from 65 to 90 %, Figure 4). The increased carbon balance during continuous operation indicates that undetected by-products were produced to a much lower level after 13 h on stream. As such, the decrease in absorbance appears to be primarily related to an increase in the selectivity of the catalyst over this period of operation.

Given that several of the products obtained by conversion of glucose are not amenable to detection by classical chromatographic means (as evidenced by the low carbon balances in Figure 2 and Figure 4), further analysis of the post-reaction effluents was undertaken by high-field liquid NMR (^{1}H-^{13}C HSQC NMR spectroscopy).[26,28] This method provides roughly 30 times higher sensitivity compared to conventional 1D ^{13}C NMR, whilst providing improved resolution due to its two-dimensional nature. As demonstrated in recent studies, [26,28] the methodology can be used to describe several products from the Lewis acid catalysed conversion of glucose, and provides an unbiased representation of by-product formation since it is also sensitive to compounds that are not easily detected with classical chromatographic methods. [26,28] The spectra of the two effluents measured by HSQC NMR (0.5 h and 13 h on stream) are shown in Figure 5.

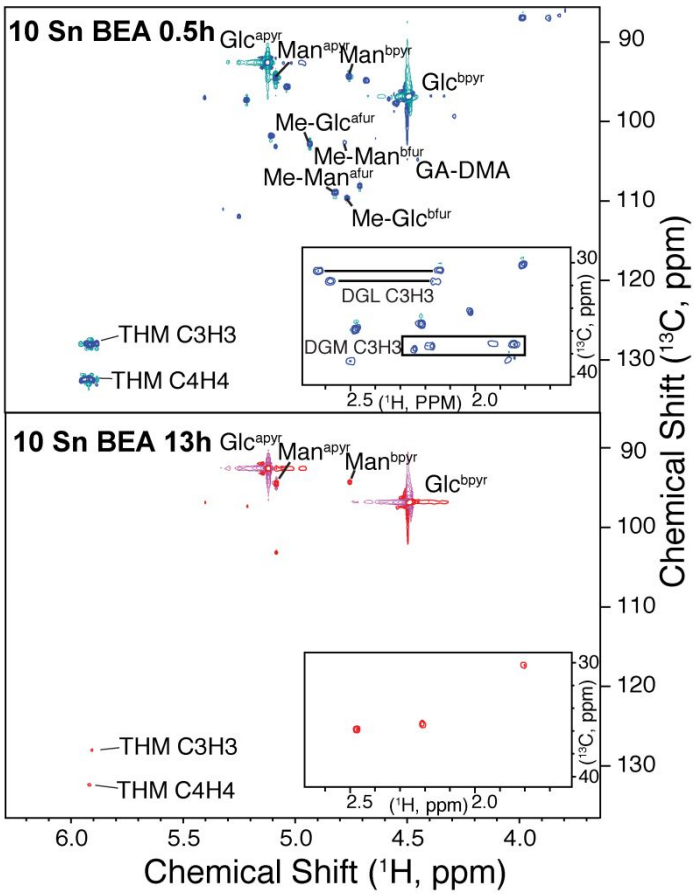

Figure 5. 2D ^{1}H-^{13}C HSQC NMR spectra of the effluent of the reactions reported in Figure 4 at 0.5 and 13 h on stream. CH groups are labelled by their position, except for C1H1 (hemi)acetal groups in carbohydrates, glycosides and aldehyde-containing furanics.

2D ^{1}H-^{13}C HSQC NMR spectra of the reaction effluent samples at 0.5 h and 13 h are displayed in Figure 5. This analysis demonstrated that the 0.5 h reaction effluent contained high quantities of THM, 3DGL, 3-deoxy-gluconic methyl ester (DGM) and furanics. According to recent studies by Tolborg *et al.*, these molecules can all be produced from β-dehydration of the same intermediate compound (3DG), which is itself formed by retro-Michael dehydration of glucose.[13] Large quantities of alkylation products (methyl-glucoside and methyl-mannoside) were also present at 0.5 hours of time on stream. Notably, the quantity of β-dehydration and alkylation products strongly decreased after 13 hours of time on stream, over the same period of time as the intensity at λ_{440} and λ_{360} decreased, and the carbon balance of the reaction increased from 65 to 90 % (Figure 4). Based on these observations, it can tentatively be ascribed that absorptions at λ_{360} and λ_{440} relate to the generation of non-selective by-products, whilst the residual λ_{330} absorption relates to selective reaction pathways (GI and/or RA),

Assignment of selective reaction pathways

To further verify these generalised assignments (λ_{330} = selective, and λ_{360} and λ_{440} = non-selective), a variety of additional *operando* UV-Vis experiments were performed. Firstly, operando UV-Vis was performed on a sample of Hf-containing zeolite Beta, which we recently demonstrated to be able to selective catalyse GI to thermodynamic equilibrium without initiating non-selective pathways.[30] We note that the basic characterisation of this material was recently published in reference 30.

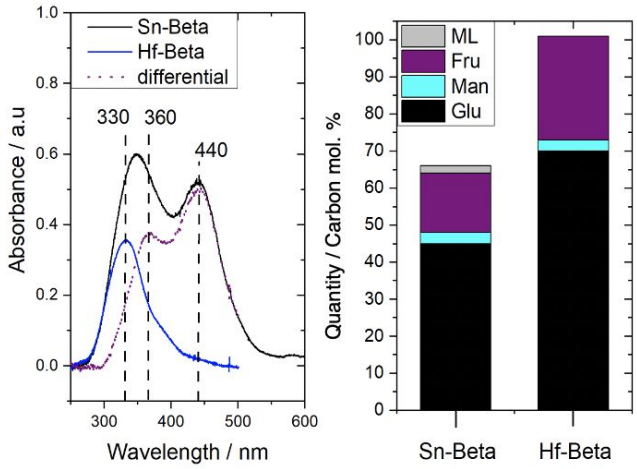

Figure 6. (Left) *Operando* UV-Vis spectra recorded during glucose conversion over Hf-Beta (blue line) and 10Sn-Beta$_{SSI}$ (black line) at 110 °C. The dotted line is the differential spectrum achieved by subtraction of the Hf-Beta spectrum from the spectrum of 10Sn-Beta$_{SSI}$. (Right) Distribution of reactant and product species in the effluent of both reactions as monitored by chromatographic methods. Reaction conditions: 1 wt. % glucose in methanol, 0.75 mL min^{-1} (Sn) and 0.65 mL min^{-1} (Hf), 0.1 g catalyst, 110 °C.

Figure 6 shows the *operando* UV-Vis spectrum generated by the catalytic conversion of glucose over Hf-Beta at 110 °C (Si/Hf molar ratio of 200), alongside the *operando* UV-Vis spectrum from the 10Sn-Beta$_{SSI}$ catalysed reaction at otherwise identical conditions. Spectra recorded at 0.5 h on stream were used for evaluation in order to be consistent with the data presented in Figure 1. We also note that Hf-Beta was first activated in a flow of methanol for 20 h prior to reaction, which we recently demonstrated to be important for activity to be observed during low temperature GI.[30] Whilst the *operando* UV-Vis spectra generated during glucose upgrading at 110°C with Sn-Beta consisted of absorbances at λ_{440}, λ_{330} and λ_{360}, the spectra from Hf-Beta did not show any absorbance at λ_{440} (Figure 6, left). Moreover, although the overall intensity of the spectrum was lower in the 330-380 nm region, this was clearly due to the absence of any major absorbance at λ_{360}, as highlighted by the differential spectrum.

Kinetic data generated during these experiments are shown in Figure 6, right. In line with our recent studies, the reaction effluent generated during the continuous conversion of glucose over Hf-Beta[30] only contained detectable quantities of glucose, fructose and mannose, with no loss of carbon balance observed. At the reaction conditions measured, the total yield of selective (GI) products when using Hf-Beta was 30 %. In contrast, at the same conditions using 10Sn-Beta$_{SSI}$ as catalyst, the level of conversion was much higher (55 % versus 30 %), but the total yield of selective products was only 24 %, confirming the poorer selectivity performance of Sn-Beta. Consequently, the carbon balance of the Sn-Beta reaction was much lower, with approximately 35 % of the initial carbon being converted into by-products not amenable to chromatographic detection. The presence of a single absorbance at λ_{330} for the catalyst exhibiting quantitative selectivity to GI and no loss in carbon balance supports assignment of the λ_{330} absorption to selective glucose conversion, and the λ_{360} and λ_{440} bands to non-selective reaction pathways.

In addition to GI, RA processes also represent a selective glucose conversion pathway. Recently, it has been reported that a key product in the RA pathway is 3DG, which is formed by retro-Michael dehydration of glucose (Scheme 1). However, in addition to being a key intermediate for RA product formation, 3DG is also a key intermediate in the non-selective β-dehydration pathway.[12,13,31] Thus, in order to aid the assignment of a signal for RA product formation, the conversion of dihydroxyacetone (DHA) to ML was studied. During this reaction, retro-Michael dehydration of DHA to pyruvaldehyde (PVA) must occur in order for ML to be produced (Scheme 2).[12,32] The reaction leading to PVA occurs *via* a pathway that is analogous to the formation of 3DG from glucose, and reportedly employs similar catalyst-substrate coordination.[12,13,33] However, this reaction cannot lead to any further β-dehydration due to the absence of a hydroxylated C_4 atom.

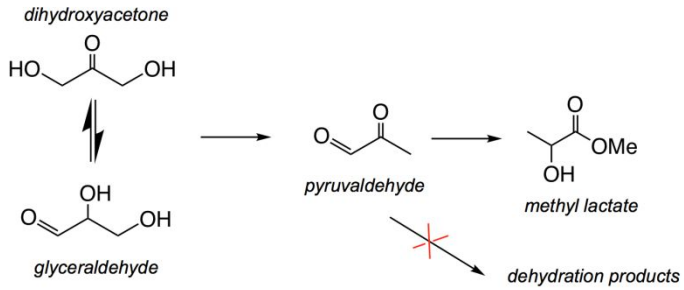

Scheme 2. Scheme of the processes related to the conversion of dihydroxyacetone to methyl lactate.

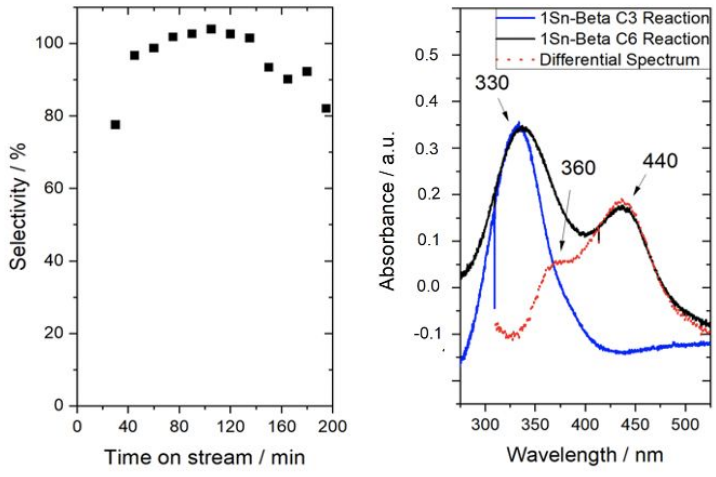

Figure 7. (Left) ML selectivity during the conversion of DHA to ML as a function of time on stream over 1Sn-Beta$_{SSI}$ at 110 °C. (Right) *Operando* UV-Vis spectra generated during the conversion of DHA to ML over 1Sn-Beta$_{SSI}$ at 110°C, compared to the spectrum generated from the analogous reaction starting from glucose. Reaction conditions: 1 wt. % glucose in methanol, 0.75 mL min^{-1}, 0.1 g catalyst, 110 °C.

The conversion of DHA to ML was performed at 110 °C with 1 % wt. Sn loaded Sn-Beta (henceforth 1Sn-Beta$_{SSI}$) as the catalyst. This catalyst was chosen since most previous works in the literature for this reaction use low loaded samples of Sn-Beta (<2 % wt. Sn).[32,34] The absence of β-dehydration pathways resulted in ML being formed at a selectivity close to 100% throughout the reaction period (Figure 7). Spectra generated by *operando* UV-Vis analysis of this reaction clearly demonstrated that the reaction was accompanied by a single absorption centred at λ_{330}, with minimal absorption evident at λ_{360} and λ_{440}. To further probe these signals, the spectrum generated at 0.5 h time on stream during the conversion of DHA to ML over 1Sn-Beta$_{SSI}$ was compared to the spectrum generated during the glucose conversion reaction at otherwise identical conditions. The red dots in Figure 7 show the difference between these two spectra, achieved by subtracting the DHA spectrum from that achieved from the glucose upgrading reaction. The differential spectrum clearly shows that the C_3 reaction primarily exhibited an intense absorption at λ_{330}, whereas the C_6 reaction exhibited a dominant signal at λ_{330}, but also significant absorptions at λ_{360} and λ_{430}. These findings support the hypothesis that the RA reaction intermediates are also embedded beneath $\lambda_{330,}$ along with the intermediates related to GI. More broadly, this analysis is indicative that the λ_{330} band relates to the coordination of Sn with the carbonyl and hydroxyl groups of the substrate molecule (*vide infra*). It is noted that whilst the spectrum of the DHA reaction still shows a slight shoulder at 360 nm, this most likely arises from the formation of traces of hexoses due to aldol condensation of two molecules of C_3, which can then be transformed by the classic glycolytic pathways shown in Scheme 1.[13]

To further aid the assignment of the optical features related to 3DG and the selective RA pathway, the effect of alkali on the reaction system was also investigated. It is widely reported in the literature that adding alkali salts to the reaction feed dramatically increases the selectivity of the glucose conversion reaction towards RA products.[13,14] Accordingly, the impact of alkali addition was evaluated for 1Sn-Beta$_{SSI}$ by recording the *operando* spectra of this catalyst in the absence and in the presence of alkali in the reaction feed. KCl (4 mg L^{-1}) was chosen as alkali additive because its wide range of effective concentration permits easier utilisation in continuous flow, and its limited basicity does not strongly impact glycoside formation in the same way as achieved by K_2CO_3, which could indirectly aid

assignment of the non-selective bands.[28] The reaction was performed at high temperature (150 °C), since the effect of alkali is more pronounced during the formation of RA products formed during the high temperature selective pathway.[28] A low loaded sample of Sn-Beta (1 wt. %) was again used for this experiment since the effect of alkali has only been confirmed for such materials.[15,32]

Figure 8 presents the *operando* UV-Vis spectra following the effect of alkali (KCl) during glucose conversion over 1Sn-Beta$_{SSI}$, alongside the kinetic data obtained in the presence and in the absence of alkali. Interestingly, in the presence of alkali, the system showed a much sharper λ_{330} absorption, a notable decrease in intensity for λ_{360}, and a very minor decrease in intensity for λ_{440}. The differential spectrum (red) of the two stages of reaction clarifies how the presence of alkali salts impacted the optical properties of the system, particularly the intensity of λ_{360}, which was minimised substantially. We note that the limited change in absorbance at 440 nm could be an early indication that this particular non-selective absorbance arises from glycoside formation, since the limited basicity of KCl has been shown to leave the alkylation pathway largely unaffected.[28]

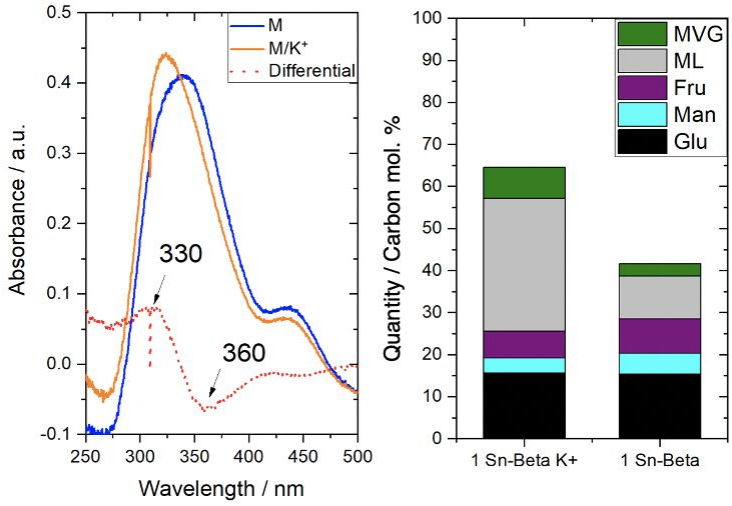

Figure 8. (Left) *Operando* UV-Vis spectra generated during the conversion of glucose by 1Sn-Beta$_{SSI}$ in the presence (orange line) and in the absence (blue line) of KCl at 150 °C (blue line). The dotted red spectrum shows the difference of these two spectra. (Right) Distribution of reactant and product species in the effluent of the reaction in the absence and presence of alkali. Reaction conditions: 1 wt. % glucose in methanol containing KCl (4 mg L^{-1}), 0.75 mL min^{-1}, 0.1 g catalyst, 150 °C.

When evaluating the impact of alkali on the kinetic performance of Sn-Beta (Figure 8, right), the most evident impact was the substantial increase of ML yield from 12 to 40 % upon inclusion of alkali. As yields to GI products and the quantity of glucose converted were largely unchanged, the carbon balance increased dramatically upon addition of alkali, suggesting that the addition of alkali led to lower quantities of by-products. The increase in the yield of RA products and increase in carbon balance was accompanied by an increase in absorbance at λ_{330} and a decrease in absorbance at λ_{360}. These findings further indicate that the optical features associated with RA formation are embedded within the λ_{330} region, and that the 360 nm region is associated with non-selective by-products.

From the data presented in this section, it is apparent that both the RA pathway (*via* 3DG) and the GI pathway are characterised by an absorbance at λ_{330}. Although each pathway would likely require the coordination of different carbonyl and hydroxyl groups, this observation can be taken as evidence that both selective pathways proceed *via* similar catalyst-substrate intermediates, which has previously been proposed in the literature but has not been supported experimentally to date.[12,13,35,36]

Assignment of non-selective pathways (λ_{440} and λ_{360})

Correlations of spectroscopic and reactivity data strongly indicate that the λ_{330} feature relates to the selective conversion of glucose, either through isomerisation or retro-aldol fragmentation, whereas the λ_{360} and λ_{440} features arise from non-selective reaction pathways. These non-selective pathways include products derived from β-dehydration and alkylation, as evidenced by chromatographic analysis and NMR spectroscopy. To better understand the nature of the λ_{360} and λ_{440} features, additional correlations were sought, with the aim of assigning both features to a specific non-selective reaction pathway.

As demonstrated in Figure 1, the two non-selective bands exhibited very different dependence on temperature. Specifically, whereas the λ_{440} feature was clearly generated at low temperature but increased only marginally with increasing reaction temperature, the λ_{360} feature was absent at low temperature but became dominant at higher temperature. Recently, Tolborg *et al.*[13] reported a study

focused upon the prevalence of by-products during the catalytic conversion of glucose over Sn-Beta between temperatures of 90-180 °C. During this investigation, the authors revealed that by-products in the low temperature regime mainly consisted of glycosidic compounds such as methyl glucopyranoside (Me-Glu) and methyl fructofuranoside (Me-Fru). Upon raising the reaction temperature beyond 110 °C, contributions from glycosidic compounds decreased, and by-products from β-dehydration and furanic production came to dominate. Graphic representation of the published data (SI Figure S8) shows how the behaviour of these two classes of compounds differed markedly with temperature. Based on this behaviour and the temperature dependences of the λ_{360} and λ_{440} features, it can be hypothesised that the low temperature λ_{440} feature arises from glycosidic pathways, whereas the high temperature absorbance at λ_{360} arises from β-dehydration. Added support for this preliminary assignment can be gained from the observation that the addition of KCl (Figure 8) decreased the magnitude of the λ_{360} feature to a much greater extent λ_{440}, which is of relevance since it has been reported that KCl does not overly impact the glycosidic reaction pathway unlike more basic alkali additives.[28]

To gain experimental support of this hypothesis, two catalysts samples were studied by *operando* UV-Vis. These included 1Sn-Beta$_{SSI}$ (prepared by post-synthetic SSI[29]) and an analogous material prepared by classical hydrothermal synthesis[37] (henceforth, 1Sn-Beta$_{HDT}$). The basic characterisation of these samples (XRD, porosimetry, ^{119}Sn MAS NMR) was recently reported in detail.[17] To obtain maximum insight from these experiments, glucose conversion was performed at 130 °C, in order to further stimulate generation of the λ_{360} feature, which only weakly contributed to the spectra at lower temperatures (Figure 9).

Figure 9 Left presents the *operando* UV-Vis spectra of glucose upgrading carried out at 130 °C by the two different samples of 1Sn-Beta, alongside the kinetic data obtained from each experiment. As can be seen, the spectrum obtained with 1Sn-Beta$_{SSI}$ was consistent with that obtained for 10Sn-Beta$_{SSI}$ at the same temperature, demonstrating a strong absorbance in the 330-380 nm region, alongside a somewhat less intense absorbance at λ_{440}. In contrast, the spectrum of 1Sn-Beta$_{HDT}$ exhibited negligible absorbance at λ_{440}, but exhibited much more intense absorbances in the 330-380 nm region.

Along with increased absorbance in the 330-380 nm region, the maximum was also clearly shifted to λ_{330} when 1Sn-Beta$_{HDT}$ was used as catalyst.

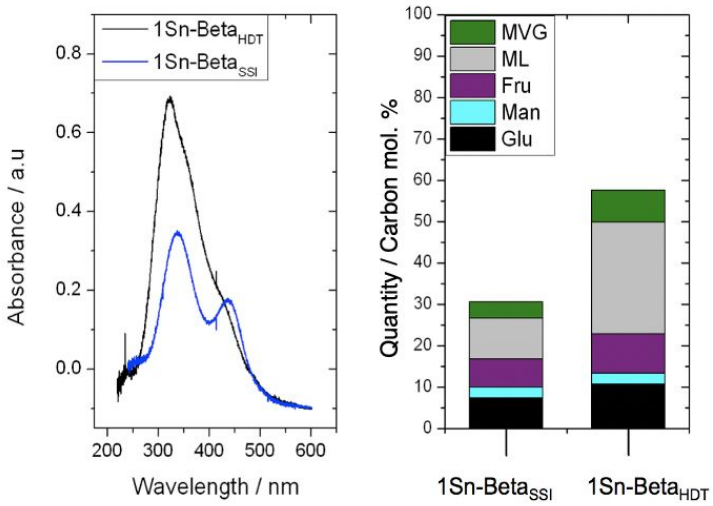

Figure 9. (Left) *Operando* spectra of the glucose upgrading reactions catalysed by 1Sn-Beta$_{SSI}$ (blue line) and 1Sn-Beta$_{HDT}$ (black line) at 130 °C, recorded at 0.5 h on stream. (Right) Distribution of reactant and product species in the effluent of the glucose conversion reaction catalysed by 1Sn-Beta$_{SSI}$ and 1Sn-Beta$_{HDT}$. Reaction conditions: 1 wt. % glucose in methanol, 0.5 mL min^{-1}, 0.1 g catalyst, 130 °C.

The product yields related to these two *operando* spectra are displayed in Figure 9, right. Whilst both experiments exhibited comparable levels of glucose conversion (*ca.* 90 %), much higher yields of selective products were obtained over 1Sn-Beta$_{HDT}$ (45 %) than over 1Sn-Beta$_{SSI}$ (22 %). This change in selectivity confirms the better performance of the hydrothermal material for conversion of glucose, in line with previous kinetic studies. In the context of this study, the higher yield of selective products obtained with 1Sn-Beta$_{HDT}$ correlates with its increased absorbance at λ_{330}, and further supports assignment of the λ_{330} feature to the selective reaction pathways. However, substantial quantities of undetected by-products were clearly produced in both cases, as evidenced by the low carbon balances observed (30 % and 70 % for 1Sn-Beta$_{SSI}$ and 1Sn-Beta$_{HDT}$, respectively). Accordingly, the effluents of these reactions were also analysed by multiplicity edited ^{1}H-^{13}C HSQC 2D NMR (Figure 10).

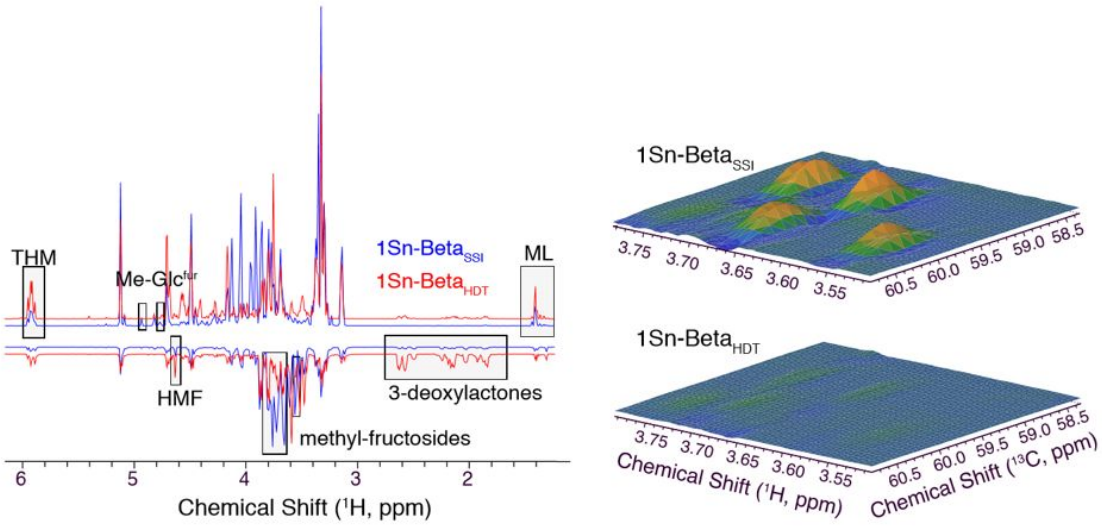

Figure 10. (Left) Positive (CH and CH_3 groups) and negative (CH_2 groups) projections from edited 2D ^{1}H-^{13}C HSQC NMR spectra recorded on the effluent of the *operando* UV-Vis glucose upgrading carried out by different preparations of Sn-Beta. (Right) Spectral region displaying signals from methyl-fructoside compounds.

Projections for the ^{1}H-^{13}C HSQC 2D spectra are shown in Figure 10, left, where positive signals derive from carbons carrying one or three hydrogen atoms, while negative intensities are derived for CH_2 groups. Signal related to Me-Glu and Me-Fru are highlighted at 4.7-4.9 ppm and at 3.6 ppm, the latter of which are shown as surface plots in the ^{1}H-^{13}C HSQC 2D spectra of Figure 10, right. It is clear that whilst 1Sn-Beta$_{SSI}$ produces substantial quantities of Me-Glu and Me-Fru at these reaction conditions, 1Sn-Beta$_{HDT}$ is less effective in producing alkyl-glycosides. In contrast, the NMR spectra reveal that 1Sn-Beta$_{HDT}$ yielded much larger quantities of lactones (2-2.5 ppm), and was much more effective at producing furanics and THM, as shown in Figure 10 (Left; signals at 5.9 ppm and 4.6 ppm). Among the non-selective absorbances (λ_{360}, λ_{440}.), 1Sn-Beta$_{HDT}$ exhibited much higher intensity in the λ_{360} region, whereas 1Sn-Beta$_{SSI}$ exhibit much larger absorption at λ_{440}. Based on these findings, absorption at λ_{360} can be attributed to by-products derived from 3DG, particularly β-dehydration products (THM, furanics) and lactones, whereas absorptions at λ_{440} can be assigned to alkyl-glycoside products.

Although each correlation is empirical in nature, the balance of evidence achieved from these mechanistic studies allows us to correlate the optical intermediates and reaction pathways of this

system in the following manner (Scheme 4): the λ_{440} arises from the formation of alkyl glycosides, which is the dominant non-selective pathway at low temperature. In contrast, λ_{360} relates to β-dehydration pathways, particularly the formation of THM and furanics, which are the major non-selective products at elevated temperature. In contrast, all selective pathways are characterised by absorbance at λ_{330}, which we believe is experimental confirmation that similar catalyst-substrate coordination occurs for all the selective glucose conversion processes (GI and RA).

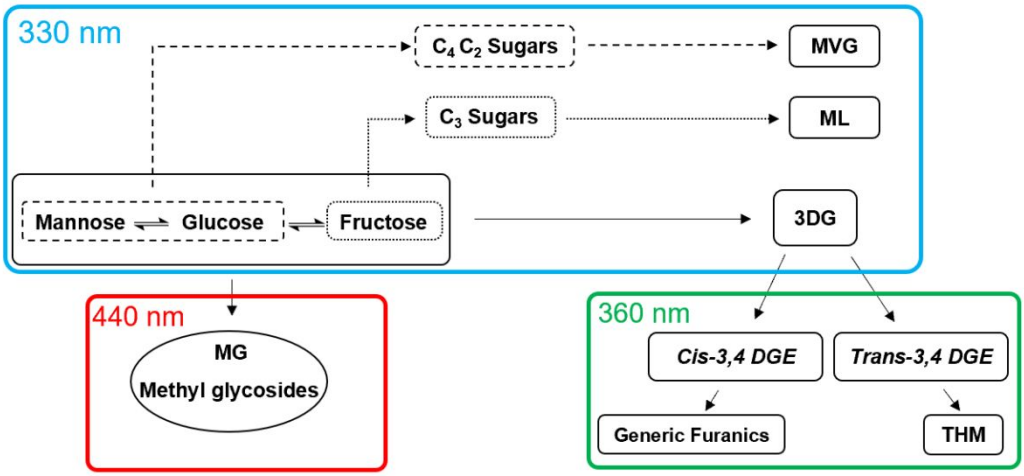

Scheme 4. Assignment of each UV-Vis absorption band to a particular glucose conversion pathway catalysed by Sn-Beta.

Use of *operando* UV-Vis to probe deactivation phenomena

Having assigned the various optical signals for intermediates that are generated during the continuous conversion of glucose over Sn-Beta (Scheme 4), the efficacy of the method to provide new information on various kinetic phenomena of the system was evaluated. In particular, the utility of *operando* UV-Vis spectroscopy to investigate the consequences of (partial) deactivation of the catalyst during continuous operation was explored.

Operando UV-Vis was therefore employed to monitor the continuous isomerisation of glucose to fructose over 10Sn-Beta$_{SSI}$ in methanol at 110 °C during a 50 h period of operation (Figure 11). The kinetic data generated during the *operando* reaction show that the system was characterized by an initially steep rate of deactivation over the first 5-10 h on stream, during which period conversion

decreased from 55 % to approximately 30 %. Over longer periods of operation, conversion continued to decrease *albeit* at a slower rate, eventually reaching a level of 15 % after 50 h on stream. Although full selectivity towards fructose was not reached even at low rates of conversion, it is notable that the selectivity of the reaction was much lower at the initial stages of operation. Analysis of the time on stream data by the Levenspiel function revealed that deactivation occurred in three distinct stages over 10Sn-Beta$_{SSI}$ at these operational conditions.[38] These stages were characterised by deactivation rate constants of 0.17 (stage 1, 0-7 h), 0.03 (stage 2, 7-25 h) and 0.01 (stage 3, 25-50 h) X%.h^{-1}.

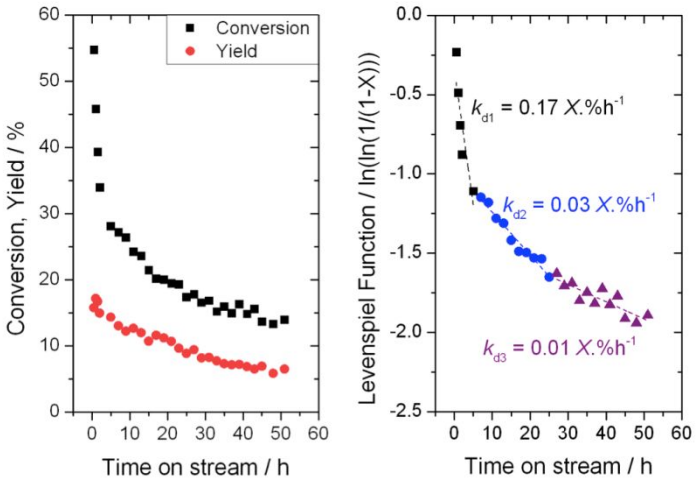

Figure 11. Kinetic data for glucose conversion over 10Sn-Beta$_{SSI}$ at 110 °C in methanol. (Left) Glucose conversion and fructose yield of the catalyst as a function of time on stream. (Right) Levenspiel function demonstrating the deactivation constant of the reaction in different stages of operation. Reaction conditions: 1 wt. % glucose in methanol, 0.75 mL min^{-1}, 0.1 g catalyst, 110 °C.

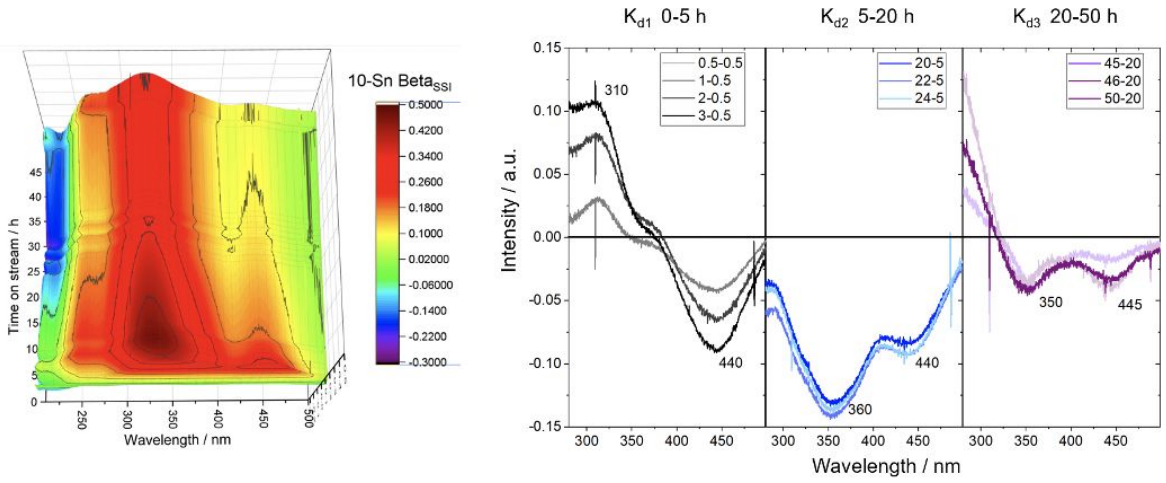

Figure 12. (Left) *Operando* UV-Vis spectrum for glucose upgrading over 10Sn-Beta$_{SSI}$ at 110 °C in methanol. Reaction conditions: 1 wt. % glucose in methanol, 0.75 mL min^{-1}, 0.1 g catalyst, 110 °C. (Right) Differential spectra for each stage of deactivation for 10Sn-Beta$_{SSI}$. In the first stage of deactivation (k_{d1}), intense loss of signal of λ_{440} is observed. In $k_{d2,}$ continued loss at λ_{440} is observed alongside strong loss of λ_{360}. In k_{d3} a more homogenous loss of λ_{340} and λ_{440} is observed.

The *operando* UV-Vis spectra generated throughout the operational period are shown in Figure 12, left in differential mode, in which the spectrum recorded prior to introducing glucose into the feed (time = 0 h), is subtracted from each spectrum. Warm colours (red) depict increased absorption relative to the fresh catalyst in methanol, whereas cold colours (blue) represent a decrease in absorption relative to the fresh catalyst in methanol.

Based on the assignments presented in Scheme 4, correlations of the *operando* UV-Vis spectra to the kinetic data were undertaken. Over the first hours on stream, conversion decreased rapidly (k_{d1} = 0.17 X%.h^{-1}) from a maximum of 55 % at 0.5 h to 28 % at 5 h on stream and the fructose yield also decreased, albeit more slowly, from 18 % to 15 %. The most evident change in the *operando* UV-Vis spectra over this time period was the large decrease in intensity of the λ_{440} feature (Figure 12, right, k_{d1}). Taken together, the rapid decrease in glucose conversion, coupled only to a minor decrease in yield but a major decrease in absorbance at λ_{440} can be ascribed to rapid deactivation of the competitive alkylation pathway, in which glucose is converted to undesirable alkylated products, such as Me-Glu, which sequesters glucose into a non-reactive form.[16]

Over the following 20 h on stream (from 5 h to 25 h), conversion continued to decrease, albeit at a slower rate (k_{d2} = 0.03 X%.h^{-1}). During this period, the selectivity of the catalyst increased gradually, as a consequence of conversion decreasing at a faster rate than yield. This observation indicates that an additional non-selective pathway was primarily deactivating in this regime. Over this time frame, a clear narrowing of the absorbance in the 330-380 nm region was observed, due to a loss of intensity at λ_{360} (Figure 12, right, k_{d2}). Increased selectivity of the catalyst alongside the decrease in intensity at λ_{360} suggests that deactivation of the β-dehydration pathways occurred during this period, resulting in decreased formation of furanics and β-dehydration products, such as THM.

Over the remaining 25 h on stream (from 25-50 h), limited changes were observed at 330 nm, suggesting that the selective pathway occurring at this temperature (GI) remains relatively unperturbed over the final period of operation. This interpretation is supported by the relatively steady time on stream data obtained during this period, during which conversion and yield decreased minimally, and reaction selectivity was unaffected. However, at this stage, a (negative) high-energy signal at 220 nm clearly increased in magnitude. As we recently reported, this signal relates to deactivation of the catalyst due to interaction with the solvent, which is the primary mechanism of deactivation for the selective pathways of the process at these operational conditions.[27] Hence, relatively slow deactivation of the selective pathway of the reaction occurs in this time frame. Taken together, *operando* UV-Vis analysis demonstrates that the deactivation of Sn-Beta during glucose conversion is non-homogeneous, and is characterised by several events occurring at different periods of time, each of which impact the activity and selectivity of the system to different degrees.

In addition to providing mechanistic insight, the findings generated by *operando* UV-Vis suggest that the catalyst becomes more selective during operation as a consequence of more rapid deactivation of the non-selective reaction pathways associated with alkylation (λ_{440}) and β-dehydration (λ_{360}). To verify if this was the case, a final kinetic experiment was performed to evaluate the selectivity of the catalyst during different stages of continuous operation (Figure 13). In this experiment, glucose conversion was performed over 10Sn-Beta$_{SSI}$ at 150 °C firstly at a flow rate of 2 mL min^{-1}. Consistent with the experiment at 110 °C (Figure 11), rapid deactivation occurred over the first 20 h of operation, with conversion decreasing from 80 % to 22 %. Over this time frame, relatively low quantities of selective products were observed in the effluent, with methyl lactate the major selective product produced at <10 % yield. After 20 h, the flow rate of the feed was decreased from 2.0 to 0.5 mL min^{-1}, thereby increasing the contact time of the reaction from 3 s to 12 s, and allowing glucose conversion to be raised back to the initial level of conversion (approximately 90 %). In doing so, it was observed that even though the quantity of glucose converted was comparable to the early stages of operation, the process was substantially more selective after 20 h on stream than during the earlier stages of reaction, with methyl lactate produced at approximately 30 % yield, versus < 10 % during the early stages of operation. The change in selectivity supports the observations made by *operando* UV-Vis,

and confirms that the catalyst becomes intrinsically more selective during continuous operation due to more rapid deactivation of the non-selective reaction pathways attributed to alkylation and β-dehydration.

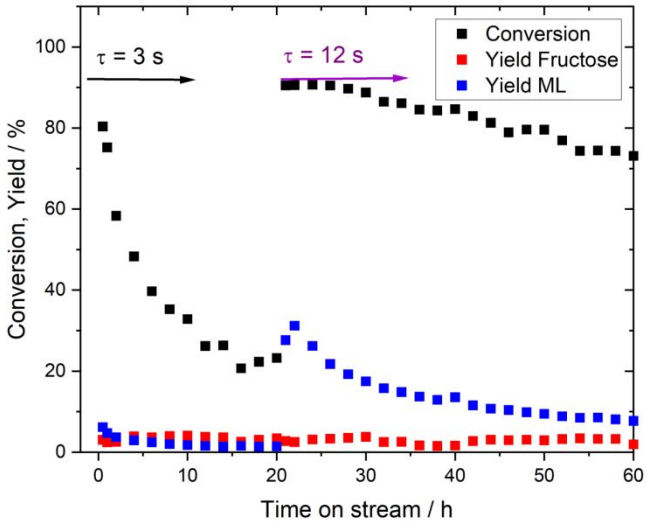

Figure 13. Kinetic data for glucose conversion over 10Sn-Beta$_{SSI}$ at 150 °C in methanol at two different flow rate regimes. Reaction conditions: 1 wt. % glucose in methanol, 0.1 g catalyst, 150 °C. Flow rate of 2 mL min^{-1} employed for first 20 h, followed by 0.5 mL min^{-1} for the remaining 40 h reaction period.

Conclusions

This study follows the catalytic conversion of glucose over the Lewis acidic silicates, Sn-Beta and Hf-Beta, at operational conditions (<150 °C, <25 bar) in a continuous flow reactor equipped with operando UV-Vis spectroscopy. Three transient absorption features related to the activation and conversion of glucose at various conditions were detected, at 330 nm, 360 nm and 440 nm. Spectroscopic (high-field ^{1}H-^{13}C HSQC NMR) and kinetic cross-experiments allow each of these Sn-glucose interactions to be assigned to a particular class of selective (330 nm, glucose isomerisation and retro-aldol products) and non-selective (360, 440 nm) products, which were found to arise from β-dehydration products (360 nm) and alkylation (440 nm) products, respectively. All selective pathways, including glucose isomerisation and retro-aldol processes, resulted in an absorbance at 330 nm, suggesting that common catalyst-substrate interactions are present during all selective reaction processes.

Based on the findings of *operando* UV-Vis, elements of the deactivation of stannosilicate catalysts during continuous operation were probed. These studies demonstrated that deactivation during glucose conversion is non-uniform, with different reaction pathways losing activity at different rates. In particular, the non-selective reaction pathway associated with alkylation (440 nm) deactivated fastest, followed by deactivation of the β-dehydration pathway (360 nm). Accordingly, the catalyst was found to increase in selectivity following partial deactivation, allowing its performance in later stages of the reaction cycle to be increased.

More broadly, the findings presented in this manuscript provide additional mechanistic insight into the glucose conversion process over Lewis acidic zeolites, and provide a new way to characterise such catalysts for biomass conversion without depending on probe molecules. In fact, although this study does not directly address the development of structure-activity relationships, it does reveal that very different catalyst-substrate interactions are observed as a function of catalyst preparation, choice of operative conditions and (partial) deactivation of the catalyst. We believe these optical features could therefore be exploited in future to unravel particular aspects of the structure-activity-lifetime relationships of Lewis acidic silicate catalysts during glucose upgrading, delivering a new tool to explore the properties of these materials and catalytic reactions.

Experimental details

Catalyst synthesis

A commercial zeolite Al-β (Zeolyst, NH_4^+-form, Si/Al = 19) was dealuminated by treatment in HNO_3 solution (13 M HNO_3, 100 °C, 20 mL g^{-1} zeolite, 20 hours). Solid-state stannation was achieved by grinding the appropriate amount of tin (II) acetate with the necessary amount of dealuminated zeolite for 10 minutes in a pestle and mortar. Following this procedure, the sample was heated in a combustion furnace (Carbolite MTF12/38/400) to 550 °C (10 °C min^{-1} ramp rate) first in a flow of N_2 (3 h) and subsequently in a flow of air (3 h) for a total of 6 h. Gas flow rates of 60 mL min^{-1} were employed at all times.

Hydrothermal synthesis of Sn-Beta was performed following a procedure described in reference 30 and 37: 30.6 g of TEOS was added to 33.1 g of TEAOH under careful stirring, forming a two-phase system. After 60–90 min, one phase was obtained and the desired amount of the tin source, typically $SnCl_4 \cdot 5H_2O$, dissolved in 2.0 mL of H_2O was added dropwise. The solution was then left for 48 h under stirring until a viscous gel was formed. The gel was finalised by the addition of 3.1 g HF in 1.6 g of demineralized H_2O yielding a solid gel with the molar composition 1.0 Si : 0.005 Sn : 0.02 Cl^{-1} : 0.55 TEA^+ : 0.55 F^{-1} : 7.5 H_2O. The obtained gel was transferred to a Teflon lined stainless steel autoclave and kept for 7 days at 140 °C to crystallise. The obtained crystals were filtered and washed with deionised water. Calcination at 550 °C (2 °C min^{-1}) for 6 h under static air was carried out in order to remove the organic template.

Kinetic studies

Continuous glucose conversion was performed in a plug flow, stainless steel, tubular reactor. The catalyst was pelletised (size fraction 63 and 77 μm) and densely packed into a ¼" stainless steel tube (4.1 mm internal diameter). Two plugs of quartz wool and a frit of 0.5 μm held the catalyst in location. Temperature control was achieved by a thermostatted oil bath held at the desired reaction temperature, and pressurization was achieved by means of a backpressure regulator. Aliquots of the reaction solutions were taken periodically from a sampling valve placed after the reactor and analysed by an Agilent 1260 Infinity HPLC equipped with a Hi-Plex Ca column and ELS detector, and quantified against an external standard (sorbitol) added to the sample prior to the injection.

NMR spectroscopy

Multiplicity-edited ^{1}H-^{13}C HSQC spectra were acquired by using a standard pulse sequence (hsqcedetgpsisp.2) on an 800 MHz Bruker Avance III NMR spectrometer equipped with a TCI z-gradient CryoProbe and a SampleJet sample changer. The spectra were obtained at 298 K by sampling 1024 and 128 complex data points in the free induction decay for acquisition times of 106 and 4.5 milliseconds in the direct (^{1}H) and indirect (^{13}C) dimensions, respectively. The indirect dimension was sampled in a traditional manner rather than by non-uniform sampling and 8 transients were averaged with an inter-scan relaxation delay of 1.2 seconds, resulting in an experiment time of ~46 minutes per

^{1}H-^{13}C HSQC experiment. All spectra were processed with a shifted sine-bell apodization function and extensive zero filling in both dimensions in Topspin 4.0.6 and analysed in the same software. Figure 10 displays positive projections of all rows in the respective two-dimensional spectra as derived with Topspin 4.0.6.

Catalyst Characterisation

Operando UV-Vis measurements were performed with a home-made tubular reactor constructed from an optically transparent material equipped with fibre optic UV-Vis probe. UV-Vis measurements were performed with a light source (Ocean Optics DH-2000), spectrometer (Maya 2000 Pro, Ocean Optics) and a 600 μm UV-Vis fibre. The light was directed onto the optically transparent reactor column, located within a heated aluminium block. A thorough explanation of the system can be found in the Supporting Information (Figures S1-S3)

Author contributions

The manuscript was written through contributions of all authors, and all authors have given approval to the final version of the manuscript.

Supporting Information

Supporting spectroscopic data are supplied in the Supporting Information.

Acknowledgements

CH gratefully appreciates the support of The Royal Society, for provision of a University Research Fellowship (UF140207, URF\R\201003) and enhanced research grant funding (RGF/EA/180314). CH and LB are grateful to Haldor Topsøe A/S for PhD studentship funding. 800 MHz NMR spectra were recorded on the spectrometer of the DTU NMR Center supported by the Villum Foundation.

References

(1) Vennestrøm, P. N. R.; Osmundsen, C. M.; Christensen, C. H.; Taarning, E. Beyond Petrochemicals: The Renewable Chemicals Industry. *Angew. Chem. Int. Ed.* **2011**, *50*, 10502–10509.

(2) Tuck, C. O.; Perez, E.; Horvath, I. T.; Sheldon, R. A.; Poliakoff, M. Valorization of Biomass: Deriving More Value from Waste. *Science*. **2012**, *338*, 695-699.

(3) Zheng, J.; Suh, S. Strategies to Reduce the Global Carbon Footprint of Plastics. *Nat. Clim. Chang.* **2019**, *9*, 374–378.

(4) Delidovich, I.; Leonhard, K.; Palkovits, R. Cellulose and Hemicellulose Valorisation: An Integrated Challenge of Catalysis and Reaction Engineering. *Energy Environ. Sci.* **2014**, *7* (9), 2803–2830.

(5) Climent, M. J.; Corma, A.; Iborra, S. Conversion of Biomass Platform Molecules into Fuel Additives and Liquid Hydrocarbon Fuels. *Green Chem.* **2014**, *16*, 516-547.

(6) Delidovich, I.; Palkovits, R. Catalytic Isomerization of Biomass-Derived Aldoses: A Review. *ChemSusChem* **2016**, *9*, 547–561.

(7) Zhang, X.; Wilson, K.; Lee, A. F. Heterogeneously Catalyzed Hydrothermal Processing of C5-C6 Sugars. *Chem. Rev.* **2016**, *116*, 12328–12368.

(8) Moliner, M.; Roman-Leshkov, Y.; Davis, M. E. Tin-Containing Zeolites Are Highly Active Catalysts for the Isomerization of Glucose in Water. *Proc. Natl. Acad. Sci.* **2010**, *107*, 6164–6168.

(9) Holm, M. S.; Saravanamurugan, S.; Taarning, E. Conversion of Sugars to Lactic Acid Derivatives Using Heterogeneous Zeotype Catalysts. *Science.* **2010**, *328*, 602–605.

(10) Dijkmans, J.; Gabriëls, D.; Dusselier, M.; de Clippel, F.; Vanelderen, P.; Houthoofd, K.; Malfliet, A.; Pontikes, Y.; Sels, B. F. Productive Sugar Isomerization with Highly Active Sn in Dealuminated β Zeolites. *Green Chem.* **2013**, *15*, 2777-2785.

(11) Moliner-Marin, M.; Roman-Leshkov, Y.; Davis, M. E.; Nikolla, E. Isomerisation of glucose to fructose by means of Lewis acid-zeolite catalysts. EP3067362A1, **2011**, *2*, 1–23.

(12) Dusselier, M.; VanWouwe, P.; deClippel, F.; Dijkmans, J.; Gammon, D. W.; Sels, B. F. Mechanistic Insight into the Conversion of Tetrose Sugars to Novel α-Hydroxy Acid Platform Molecules. *ChemCatChem* **2013**, *5*, 569–575.

(13) Tolborg, S.; Meier, S.; Sádaba, I.; Elliot, S. G.; Kristensen, S. K.; Saravanamurugan, S.; Riisager, A.; Fristrup, P.; Skrydstrup, T.; Taarning, E. Tin-Containing Silicates: Identification of a Glycolytic Pathway via 3-Deoxyglucosone. *Green Chem.* **2016**, *18*, 3360–3369.

(14) Tolborg, S.; Sádaba, I.; Osmundsen, C. M.; Fristrup, P.; Holm, M. S.; Taarning, E. Tin-Containing Silicates: Alkali Salts Improve Methyl Lactate Yield from Sugars. *ChemSusChem* **2015**, *8*, 613–617.

(15) Padovan,D.; Tolborg,S.; Botti,L.; Taarning,E.; Saḍaba,I.; Hammond, C. Overcoming Catalyst Deactivation during the Continuous Conversion of Sugars to Chemicals: Maximising the Performance of Sn-Beta with a Little Drop of Water. *React. Chem. Eng*. 2018, 3, 155−163.

(16) Tosi, I.; Riisager, A.; Taarning, E.; Jensen, P. R.; Meier, S. Kinetic Analysis of Hexose Conversion to Methyl Lactate by Sn-Beta: Effects of Substrate Masking and of Water. *Catal. Sci. Technol.* **2018**, *8*, 2137–2145.

(17) Botti, L.; Navar, R.; Tolborg, S.; Martinez-Espin, J. S.; Padovan, D.; Taarning, E.; Hammond, C. Influence of Composition and Preparation Method on the Continuous Performance of Sn-Beta for Glucose-Fructose Isomerisation. *Top. Catal.* **2019**, *62*, 1178–1191.

(18) Wolf, P.; Liao, W. C.; Ong, T. C.; Valla, M.; Harris, J. W.; Gounder, R.; van der Graaff, W. N. P.; Pidko, E. A.; Hensen, E. J. M.; Ferrini, P.; et al. Identifying Sn Site Heterogeneities Prevalent Among Sn-Beta Zeolites. *Helv. Chim. Acta* **2016**, *99*, 916–927.

(19) Hammond, C.; Padovan, D.; Al-Nayili, A.; Wells, P. P.; Gibson, E. K.; Dimitratos, N. Identification of Active and Spectator Sn Sites in Sn-β Following Solid-State Stannation, and Consequences for Lewis Acid Catalysis. *ChemCatChem.* **2015**, *7*, 3322–3331.

(20) Yakimov, A. V.; Kolyagin, Y. G.; Tolborg, S.; Vennestrøm, P. N. R.; Ivanova, I. I. ^{119}Sn MAS NMR Study of the Interaction of Probe Molecules with Sn-BEA: The Origin of Penta- and Hexacoordinated Tin Formation. *J. Phys. Chem. C* **2016**, *120*, 28083–28092.

(21) Gunther, W. R.; Michaelis, V. K.; Griffin, R. G.; Roman-Leshkov, Y. Interrogating the Lewis Acidity of Metal Sites in Beta Zeolites with 15N Pyridine Adsorption Coupled with MAS NMR Spectroscopy. *J. Phys. Chem. C* **2016**, *120*, 28533–28544.

(22) Boronat, M.; Concepción, P.; Corma, A.; Renz, M.; Valencia, S. Determination of the Catalytically Active Oxidation Lewis Acid Sites in Sn-Beta Zeolites, and Their Optimisation by the Combination of Theoretical and Experimental Studies. *J. Catal.* **2005**, *234*, 111–118.

(23) Harris, J. W.; Cordon, M. J.; Di Iorio, J. R.; Vega-Vila, J. C.; Ribeiro, F. H.; Gounder, R. Titration and Quantification of Open and Closed Lewis Acid Sites in Sn-Beta Zeolites That Catalyze Glucose Isomerization. *J. Catal.* **2016**, *335*, 141–154.

(24) Yakimov, A. V.; Kolyagin, Y. G.; Tolborg, S.; Vennestrøm, P. N. R.; Ivanova, I. I. ^{119}Sn MAS NMR Study of the Interaction of Probe Molecules with Sn-BEA: The Origin of Penta- and Hexacoordinated Tin Formation. *J. Phys. Chem. C* **2016**, *120*, 28083–28092.

(25) Vimont, A.; Thibault-Starzyk, F.; Daturi, M. Analysing and understanding the active site by IR spectroscopy. *Chem. Soc. Rev.* **2010,** *39,* 4928-4950.

(26) Meier, S. In-Situ Annotation of Carbohydrate Diversity, Abundance, and Degradability in Highly Complex Mixtures Using NMR Spectroscopy. *Anal. Bioanal. Chem.* **2014**, *406*, 7763–7772.

(27) Padovan, D.; Botti, L.; Hammond, C. Active Site Hydration Governs the Stability of Sn-Beta during Continuous Glucose Conversion. *ACS Catal.* **2018**, *8*, 7131–7140.

(28) Elliot, S. G.; Tolborg, S.; Sádaba, I.; Taarning, E.; Meier, S. Quantitative NMR Approach to Optimize the Formation of Chemical Building Blocks from Abundant Carbohydrates. *ChemSusChem* **2017**, *10*, 2990–2996.

(29) Hammond, C.; Conrad, S.; Hermans, I. Simple and Scalable Preparation of Highly Active Lewis Acidic Sn-β. *Angew. Chem. Int. Ed.* **2012**, *51*, 11736–11739.

(30) Botti, L.; Kondrat, S. A.; Navar, R.; Padovan, D.; Martinez-Espin, J. S.; Meier, S.; Hammond, C. Solvent-Activated Hafnium-Containing Zeolites Enable Selective and Continuous Glucose–Fructose Isomerisation. *Angew. Chemie - Int. Ed.* **2020**, *59,* 20017–20023.

(31) Assary, R. S.; Curtiss, L. A. Comparison of Sugar Molecule Decomposition through Glucose and Fructose: A High-Level Quantum Chemical Study. *Energy and Fuels* **2012**, *26*, 1344–1352.

(32) Taarning, E.; Saravanamurugan, S.; Holm, M. S.; Xiong, J.; West, R. M.; Christensen, C. H. Zeolite-Catalyzed Isomerization of Triose Sugars. *ChemSusChem* **2009**, *2*, 625–627.

(33) Dusselier, M.; De Clercq, R.; Cornelis, R.; Sels, B. F. Tin Triflate-Catalyzed Conversion of Cellulose to Valuable (α-Hydroxy-) Esters. *Catal. Today* **2017**, *279*, 339–344.

(34) Chang, C. C.; Wang, Z.; Dornath, P.; Je Cho, H.; Fan, W. Rapid Synthesis of Sn-Beta for the Isomerization of Cellulosic Sugars. *RSC Adv.* **2012**, *2*, 10475–10477.

(35) Yang, G.; Pidko, E. A.; Hensen, E. J. M. The Mechanism of Glucose Isomerization to Fructose over Sn-BEA Zeolite: A Periodic Density Functional Theory Study. *ChemSusChem* **2013**, *6*, 1688–1696.

(36) Elliot, S. G.; Taarning, E.; Madsen, R.; Meier, S. NMR Spectroscopic Isotope Tracking Reveals Cascade Steps in Carbohydrate Conversion by Tin-Beta. *ChemCatChem* **2018**, *10*, 1414–1419.

(37) Tolborg, S.; Katerinopoulou, A.; Falcone, D. D.; Sadaba, I.; Osmundsen, C. M.; Davis, R. J.; Taarning, E.; Fristrup, P.; Holm, M. S. Incorporation of Tin Affects Crystallization, Morphology, and Crystal Composition of Sn-Beta. *J. Mater. Chem. A* **2014**, *2*, 20252–20262

(38) Levenspiel, O. *Industrial & Engineering Chemistry Research*; 1999; 38, 4140-4183.

Table of contents graphic